Application of Dynamical Mechanical Analysis and Rheometry for Measuring Dwell Time in FastForm® Pattern Wax

Originally published
2013

Remet UK Limited
Robert J Brown
Remet Corporation
Joe Stanco

1. Abstract

The Remet FastForm® range of injectable waxes were designed to set up rapidly and are ideally suited for increasing productivity when injecting large patterns such as those found in precision investment cast pumps and valve bodies used in oil and gas industries. Initial results of DOE studies carried out with an MPI wax injector showed a marked decrease in cycle time while maintaining dimensional and surface finish quality comparable to standard wax. Establishing acceptable injection parameters for each wax injector often requires large number of samples to be injected. Thermophysical instrumentation offers methods independent of injection machine for characterizing these parameters. Differential scanning calorimetry (DSC) has been used to examine the crystallization and solidification of wax and wax components. DMA (Dynamic Mechanical Analysis) has been used to characterize solid shrinkage of wax. We have previously reported on the potential for controlled stress rheometry (CSR) and DMA as investigative tools to look at the viscoelastic properties of waxes across the solid/liquid phase boundary. These investigative approaches were correlated with results obtained with the MPI injector. This composite approach permits a potential user of pattern waxes such as FastForm® to quickly establish injection parameters from a reduced number of test injections.

2. Introduction – Taking Science into the Wax Room

2.1 Background

Many of you, reading this, will think that the title of this section is absurd! – We already have Science in the wax room. After all, what else are all the injection trials, DOE matrices, statistical analyses and data gathering about?

Even the injection presses now seem to do Science by themselves, gathering digital data on each injection and squirreling it away for regular analysis. Phipps [1] reported on data collection and analysis of key metrics from the wax injector as major drivers to more robust control and higher throughput of wax patterns with improved quality and consistency.

But Science has been defined in some volumes as not only the gathering of knowledge, but it's organisation into a form of testable explanations and predictions about the universe. In this paper we hope to be able to establish explanations, and perhaps predictions for properties engineered into a group of wax formulations.

One such group of waxes, Remet's FastForm® family of pattern waxes, is formulated to reduce cycle time at low shrinkage rate with excellent surface finish quality.

As Monk [2] points out, it is common practice to measure the viscosities of molten wax over wide range of temperatures to establish appropriate range of injection temperatures. However, it is exceedingly difficult to measure their viscosity at or near the congealing point using conventional techniques. How and why the optimized wax behaves near its congealing temperature is the subject of this paper and it is hoped that by the end we will all have a better appreciation of what is going on within the wax, and indeed how to get the most out of it for developing faster setting pattern waxes.

2.2 The Origins of FastForm®

Yield and productivity are the essence of survival in manufacturing. In any production environment, the difference between a successful business and a failing one can sometimes come down simply to the amount of production achieved (or indeed achievable) from the initial capital investment.

If we consider then the wax room, business management dictates that any successful capital investment such as wax injection presses provide a sound ROI including. Ideally, the presses should be kept continually pumping wax into the tools, and the tools themselves should be cycling through pattern after pattern to feed the rest of the production line with near zero defects.

Where the involved processes are active they have been effectively optimized. Presses inject quickly, tools are designed to be filled efficiently, and removal of injected patterns has even been subjected to robotic efficiency. These processes are driven to the greatest efficiency we can manage.

With passive processes, the optimization is more limited, as they can't be driven. We can improve heat flow in a material for example by increasing the gradient across which the heat may be flowing, but while heat can be pumped in quite simply, coldness cannot. We are restricted to removing the heat which is present. We can boil soup in a microwave in seconds, whilst making ice cream and sorbet still takes a lot longer.

In the wax room then, a process step which may restrict productivity is the dwell time, that is, the time required to fill the die and for the injected pattern to cool sufficiently under wax pressure before being extracted and the tool re-used.

This is especially acute with large parts having thick sections where the dwell time might actually be defined from the heat capacity and thermal conductivity of the wax rather than the efficiency with which the tool is cooled.

FastForm® pattern waxes, in particular, FastForm 20F is a low volume fraction (<20%) filled pattern wax designed to provide comparable dimensional stability at reduced dwell time compared to higher (30-40%) filled waxes while reducing the propensity for shell cracking.

3. Objective - So what are we going to measure?

As previously reported [3], Remet UK presented results from rheology measurements during cooling of wax and examined the viscoelastic properties by dynamic mechanical analysis (DMA). This year we have used the same instrumentation, albeit with some slightly different methods to explore where we've got to with "FastForm®" and how the optimized formulation works.

The sampling of the product to the UK laboratory was deliberately provided without any product specification so that our set up and running of the instruments would not be biased by any pre-assumption of the results.

The new "FastForm" product, was compared with one of Remet Corporations's standard line of filled wax products, Wax B – which is a 30% bisphenol A (BPA) filled wax, and an alternative Wax C which is 40%t terephthalic acid (PTA) filled wax.

3.1.1 Rheometry

One of the key limitations with many wax formulations is the rise in viscosity as the waxes approach their respective softening points. With the rheometer we can measure the viscosity down towards the softening point and chart the development of non-Newtonian flow characteristics as the temperature falls. It might be imagined that a wax with a short dwell time could show variation from regular wax in terms of the viscosity close to the softening point.

Earlier studies [3] demonstrated how fast temperature control a controlled stress rheometer instrument with Peltier plate thermostat system can show differences in wax behavior.

3.1.2 Dynamical Mechanical Analysis (DMA)

Since last year we have been examining the free contraction of a wax in the solid phase with the DMA. This method had proven to be a useful analytical tool as it represents the shrinkage of the wax after the injection has stopped when the wax begins freezes off, i.e. beyond the influence of press settings.

This contraction is also a measure of how much of the crystalline component of a blended wax remains in amorphous or liquid form (i.e. un-contracted).

3.1.3 Differential Scanning Calorimetry (DSC)

While DSC is a well-established instrumental technique familiar to many within the PIC industry, a few years ago the scientists working within the Perkin Elmer company on applications of the Power Compensated DSC technique realized that certain historical limits for their DSC instruments simply did not apply.

As shown schematically in Figure 3.1, difference between the two instrument designs is that a flux-plate DSC has both sample and reference pan in the same furnace, where the power compensated design has a furnace for each pan.

Figure 3.1 Comparison of heat flux (top) and power compensated DSC designs

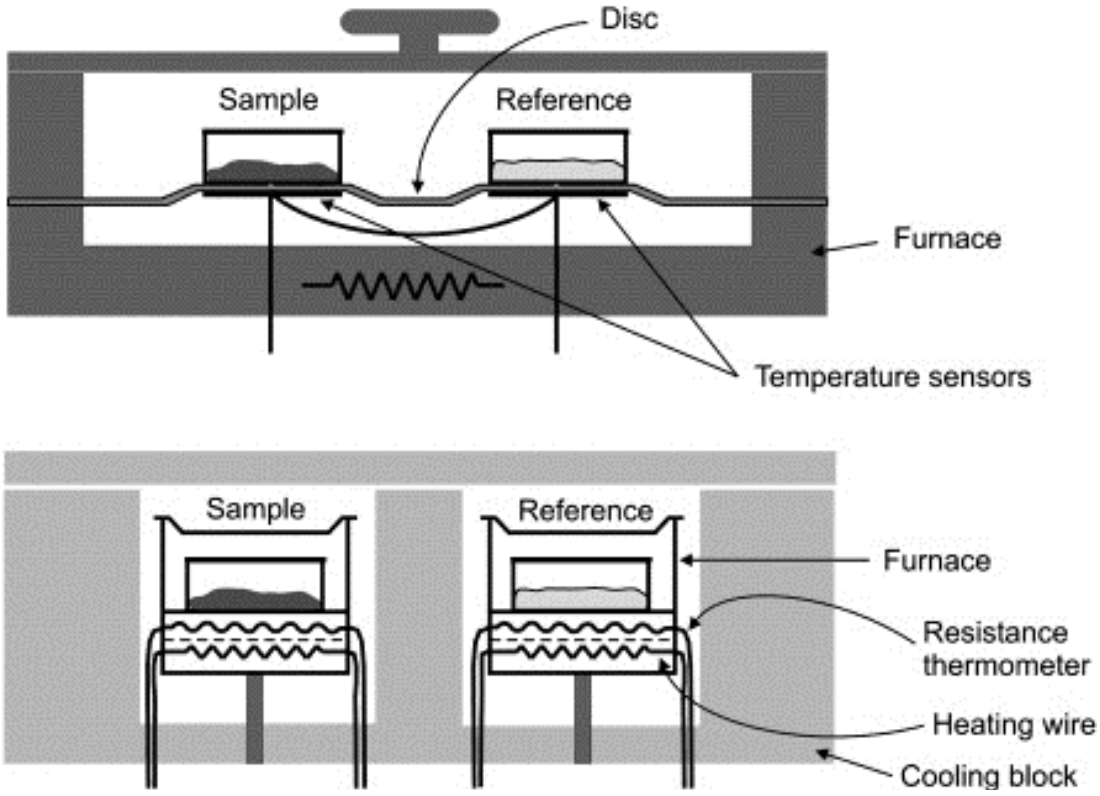

Thus with heat flux DSCs the samples are in the same environment and the temperature difference between sample and reference are measured while power compensation records the energy required to keep the samples at the same temperature.

Traditionally DSC experiments both on flux-plate and power compensated instruments were carried out at pedestrian scanning rates of 1, 5 and 10 oC/ minute with the occasional use of 20 oC/minute to elucidate the occasional difficult Tg. For many years, the users of power compensated instruments merely used the faster scanning rate capability of the instruments to get from one fixed temperature to another.

The realization that these instruments were actually capable of collecting useful data at these higher speeds has led to the development of various methods collectively known as Hyper-DSC.

Thankfully even older power compensated instruments are capable of reaching some of these speeds meaning we can collect data at least up to 40oC/minute, a scanning rate much closer to the reality of a wax cooling after injection!

4. Materials and Methods – Getting the data out of the wax

4.1 Rheometry experiments.

A sample of each of the waxes we tested was placed on the Peltier plate of a Brookfield Instruments RS+ Controlled Stress Rheometer equipped with a 50 mm flat plate spindle gapped to 0.5 mm.

Each sample was conditioned at 110 oC for two minutes at a shear rate of 20 1/s. The samples were then ramped down to their respective softening points over a 300s period. Each sample was then re-heated to 110oC, conditioned again and then cooled over a 200 s period. Again the sample was reheated and finally cooled over a 100 s period, the resulting curves being plotted as an overlay.

4.2 DSC Experiments.

The DSC experiment was set up in a format widely used for waxes, where the sample is held initially in a completely molten state (110oC), cooled to room temperature or below (in this instance 0 oC is used to guarantee completeness of solidification) and then ramped back to 110 oC.

Where the method here is slightly different is that the ramp cycle is repeated at different cooling rates i.e. 10, 20, 30, and 40 oC/m and held for 2 m at 110oC

The heating data is discarded as we are primarily interested in cooling and, the cooling traces are overlaid for comparison.

4.3 DMA Experiments.

DMA instruments are renowned for their flexibility and adaptability, and the Triton Technologies TTDMA is no exception. Previously [3], the instrument was configured to use folded steel sample pockets for viscoelastic measurements.

For the work presented here, the instrument was set up in compression mode, and used statically, essentially as a very “light touch” micrometer in a temperature controlled environment.

Figure 4.1 DMA Compression assembly.

Each sample of wax was prepared as a 9 mm nominal square section of wax which was inserted between the plates of the compression mode assembly as shown in Figure 4.1. The temperature control was then cycled up close to the softening point of the test wax so that the sample embedded onto the assembly to guarantee consistent dimensions and parallel plates. Figure 4.2 presents an example of the embedding portion of the DMA cycle.

Figure 4.2. DMA trace for embedding of wax onto sample fixture.

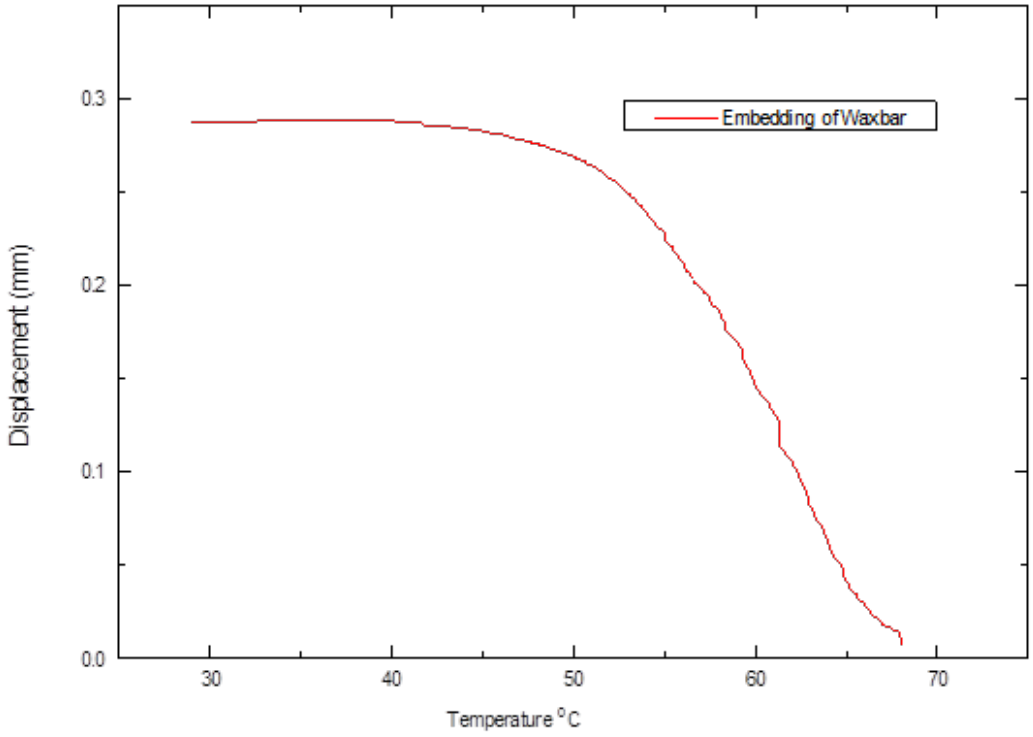

As can be seen from the figure, the embedding process leaves the static displacement within 0.007 mm of the instrument's "neutral" position. (where the assembly rests in the absence of any applied force). A static upwards force of 0.005 N is applied to ensure the sample remains in good contact with the plates throughout the experiment.

Once the sample is embedded and in contact with the compression assembly, it was cooled slowly back towards room temperature. As the embedding process takes place at the maximum expansion of the wax, there are no compressive forces acting on the sample throughout the subsequent steps of the experiment. The contraction is completely free.

The entire heating and cooling cycle is then repeated to allow for both repeatability of the cooling and the hysteresis of the sample's dimensional changes to be observed. An example trace is shown below:

Figure 4.3 Expansion/contraction cycles showing hysteresis and repeatability.

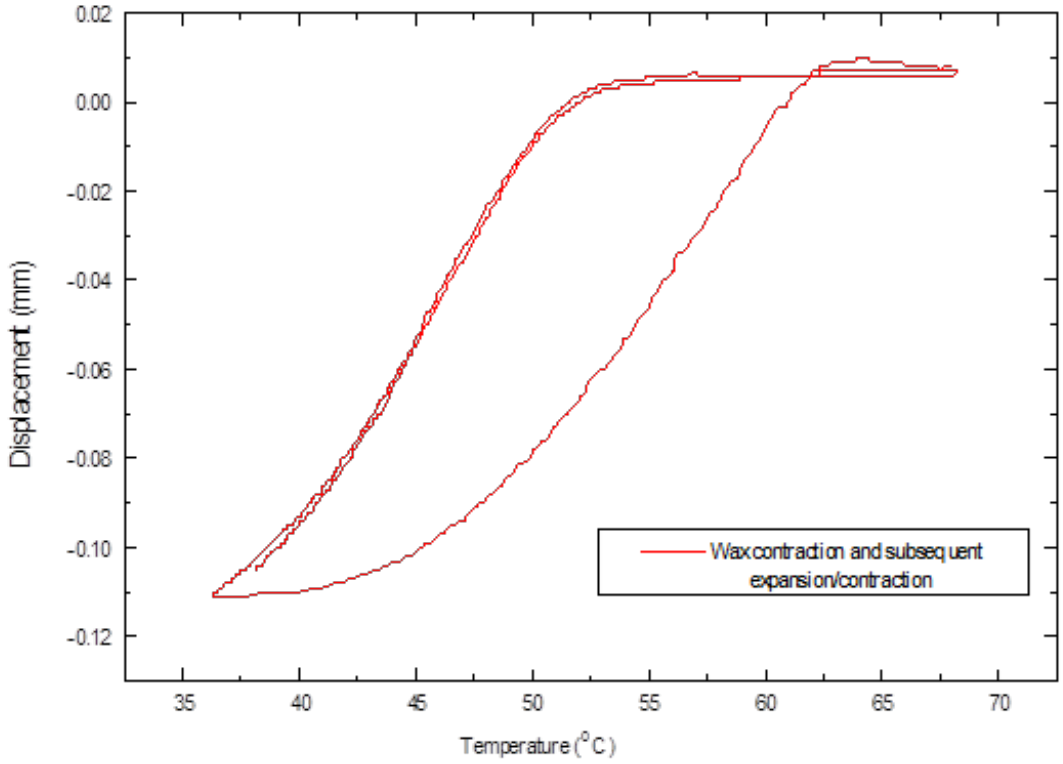

At the end of an experiment, the embedding step served to normalise the sample size and the expansion curves can be compared directly. A nominal 9 mm thick sample generally ends up with a final thickness of 8.56 mm.

4.4 Wax Injection through Design of Experiment (DOE)

Since FastForm is a new family of wax developed at Remet, a DOE similar to that conducted by Phipps [1] was carried out on a 25 ton MPI 55-25-24 wax injector to evaluate data as well as develop dimensional prediction formula. As presented in Figure 4.4, the DOE considered the interaction between wax temperature, injection pressure and dwell time with wax flow held constant. Wax tested included both unfilled and nominally 20% filled FastForm waxes along with a Remet standard 20% BPA filled Wax B. Wax C was not available for this portion of the experiments. All waxes were injected into long thin bars (11.8 L x 1 W x 0.125 T). All data was collected and analysed to determine effects each parameters had on dimension and to determine the optimum injection parameters required to obtain desired dimension with the lowest dwell time.

Figure 4.4. DOE for injecting wax considers interaction between wax temperature, injection pressure and dwell time.

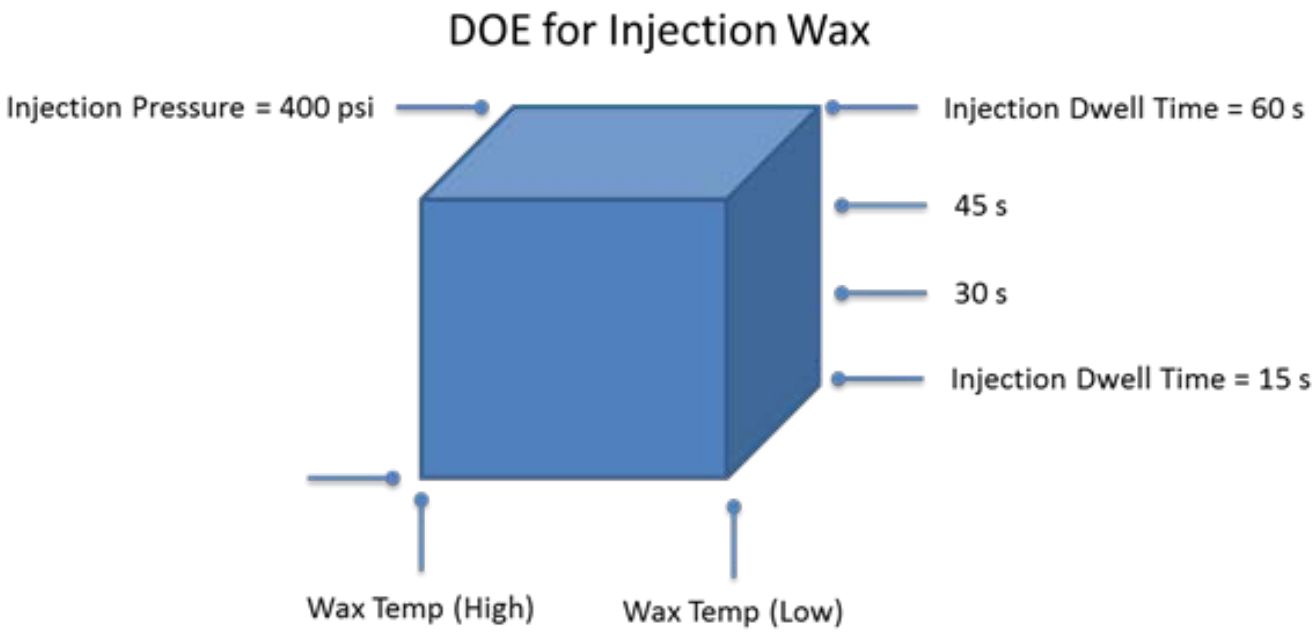

5. Results and Discussion – What can we learn?

5.1 Results from Controlled Stress Rheometry

Looking at the graph of Figure 5.1 obtained from Wax B, the pattern familiar to readers of last year's paper emerges where it can be seen that non-Newtonian flow develops in the wax as it is cooled from molten towards the softening point. Increasing the cooling rate produces a "lag" in viscosity increase typical of a variable crystallisation processes occuring, though it cannot be determined whether the rheological change is prompted by the quantity of material crystallising or by the crystal size.

The experiment was halted with at the softening point for the wax as the lowest point given the trend was clearly visible, and the faster cooling rates lose resolution when there is a rapid change in measured viscosity.

The rheological behaviour of Wax C presented in Figure 5.2 also shows some non-Newtonian behaviour, albeit evolving at a lot lower rate. The increase in viscosity towards the softening point is much less pronounced, and the lower lag time suggests either a different crystallisation process, or less variation in the crystallites produced by different cooling speeds.

Figure 5.1. Rheology curves of FastForm 20F at different cooling rates.

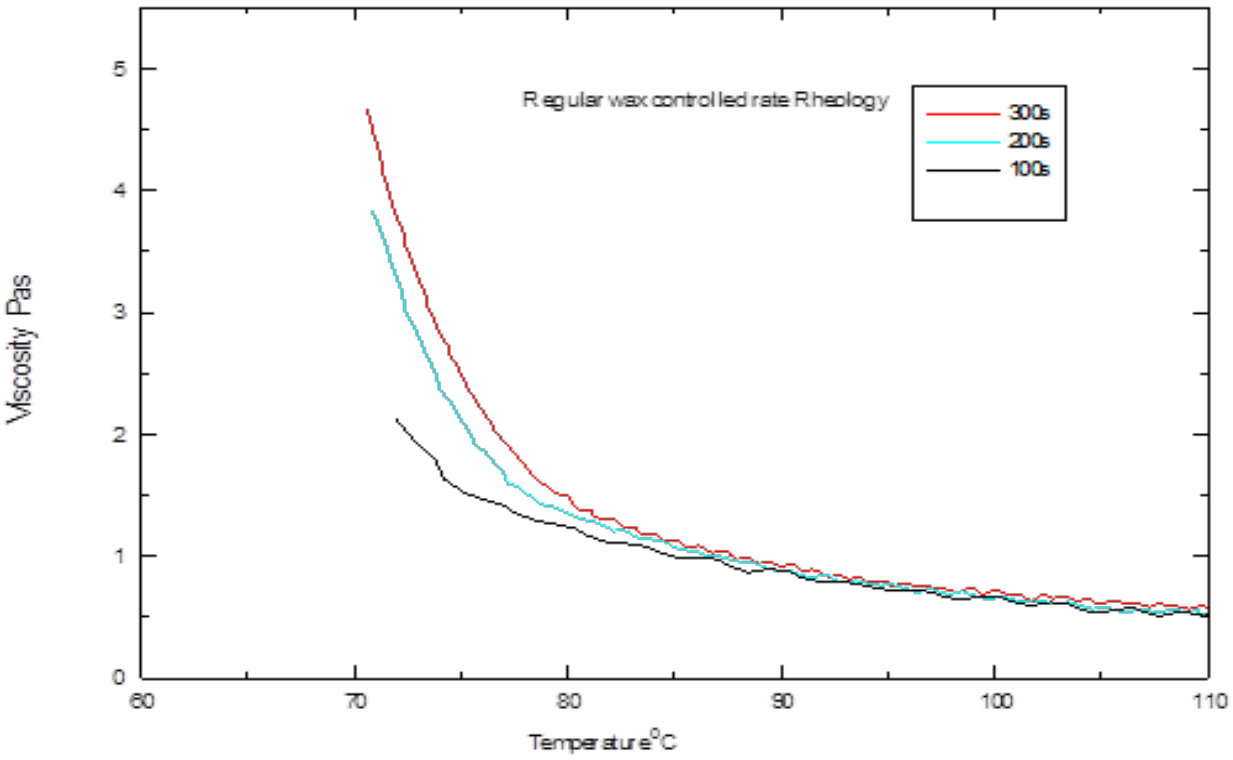

Figure 5.2 Rheology curves from cooling Wax B at different rates.

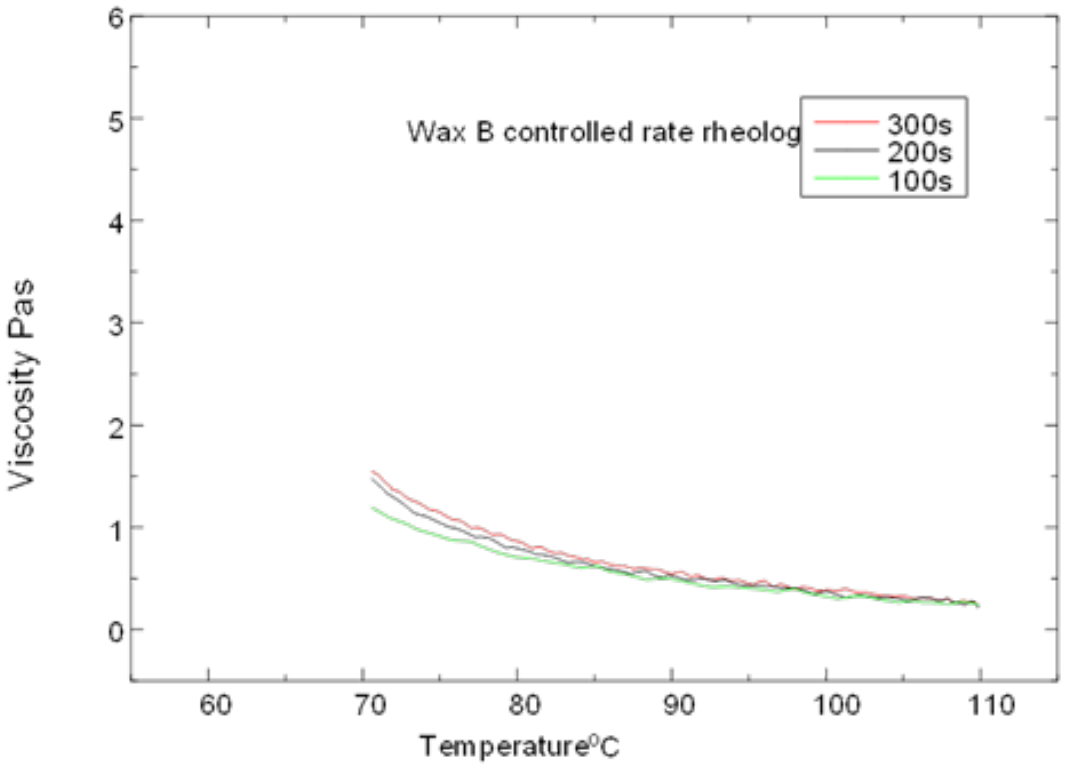

This lag time effect is even less evident in the results obtained from FastForm 20F. Note that all of the waxes are shown on the same viscosity scale for comparability and that each wax was only recorded as far as the recorded softening point from the data sheet.

Figure 5.3. Rheology curves from cooling Wax C at different rates.

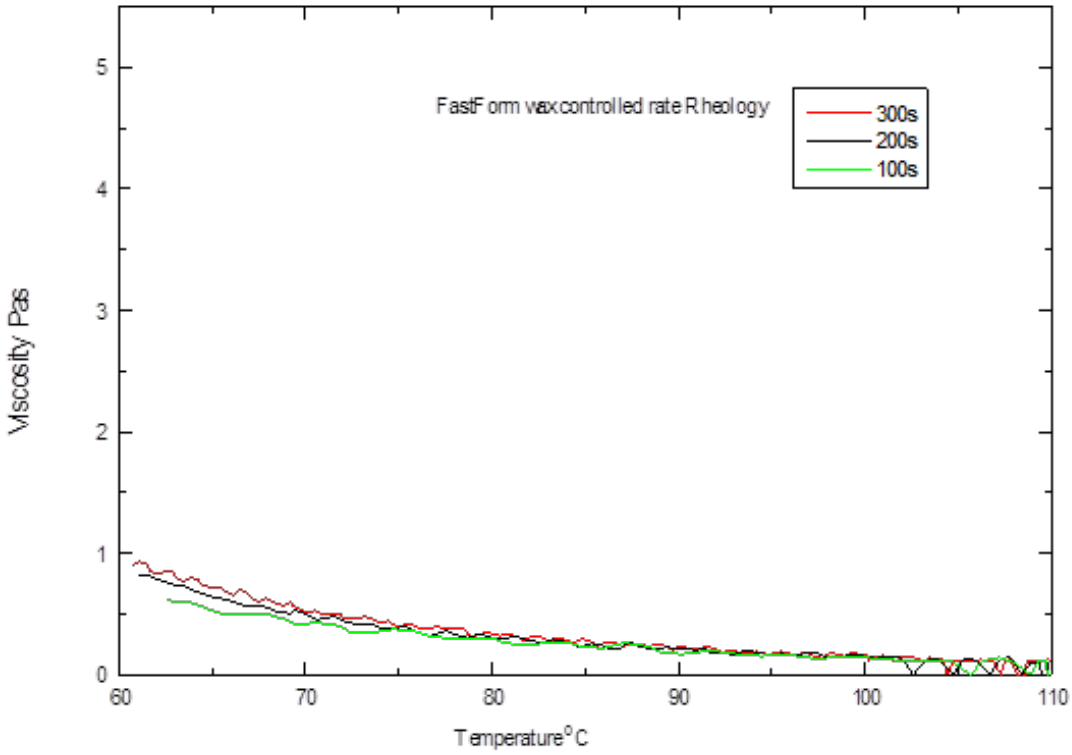

It should be noted that the softening point of FastForm is lower than the softening points of either Wax B, or Wax C (which are both similar at 71.1oC and 70.8oC respectively). Nevertheless, the evolution of non-Newtonian characteristics clearly occurs less at the softening point of FastForm 20F than with either of the other two waxes tested.

It might be predicted then that for injection of FastForm 20F at a given viscosity, not only would the temperature of injection be lower, but the wax would flow into the tool equally as well or better than the other waxes, even were they employed at the higher temperature. Furthermore, it might also be predicted that the less variable crystallization process will produce a more reliable and repeatable set-up time.

5.2 Results from DSC Experiments.

The DSC experiment carried out provided further insights on the effects of variable cooling rates on the crystallisation of the wax. Exothermic transitions on cooling would normally be caused either by crystallisation of material from an amorphous matrix, or solid-solid rearrangement of crystals to a lower energy state. The latter would be slower and less energetic than new crystallisation. Since Wax B consists of multiple crystallizing components, Figure 5.4 suggests two exothermic stages for the cooling as reflections of different materials crystallising from the wax.

Figure 5.4. DSC traces from cooling of Wax B at different cooling rates.

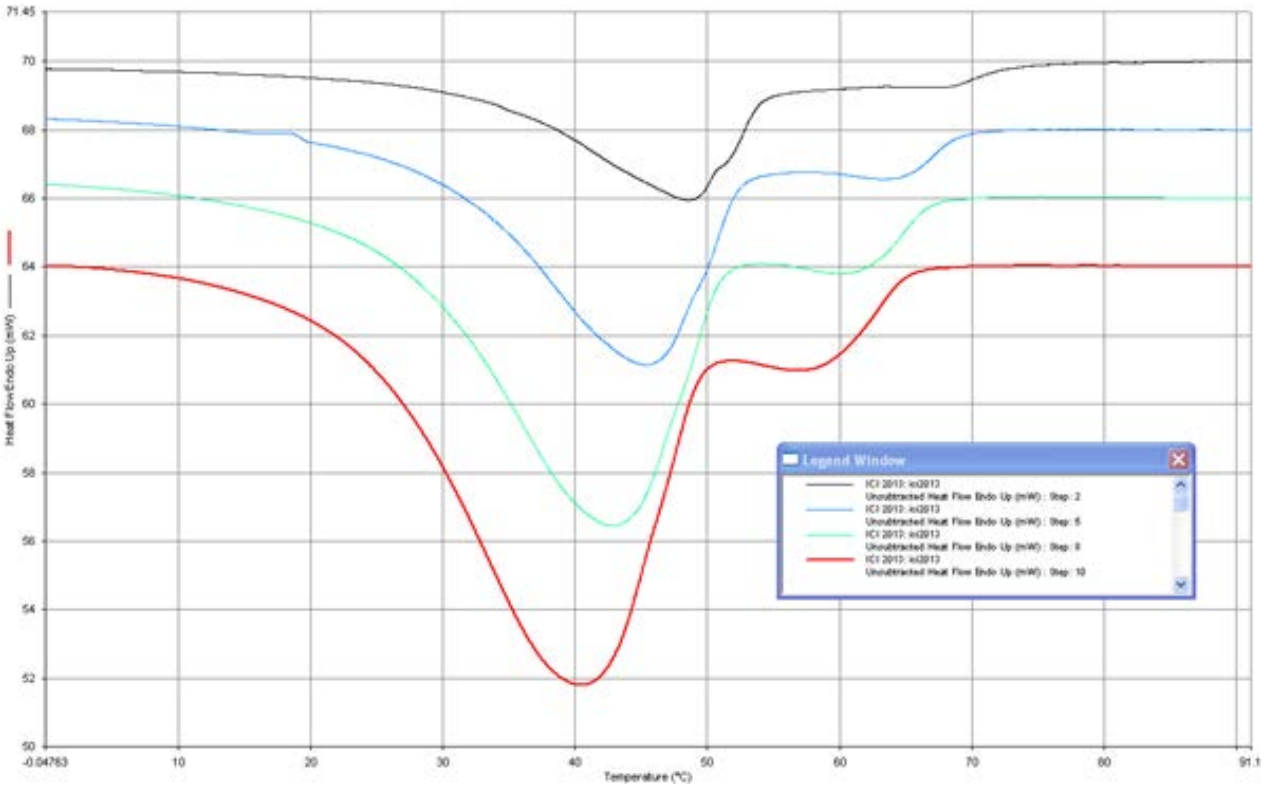

Again, what is clearly visible is that at faster cooling rates, the major crystallisation peak moves to a lower temperature. (The intensity of the recorded peak is affected by the enhanced sensitivity of the DSC instrument at faster scanning rates). Interestingly, the drastic rise in viscosity towards the melting point can be attributed to the crystallisation of a minor formulation component, as it occurs at far higher temperature than the bulk of the crystallisation.

Comparing this with the DSC curve for Wax C in Figure 5.5 is that the same displacement effect for the position of the main exotherm occurs, but that the exotherm occurs 10oC earlier in the cooling, despite the products having a similar softening point. This particular product also exhibits a far more homogenous crystallisation process with less evidence for discreet crystallisation stages.

Figure 5.5. DSC traces from cooling of Wax B at different cooling rates.

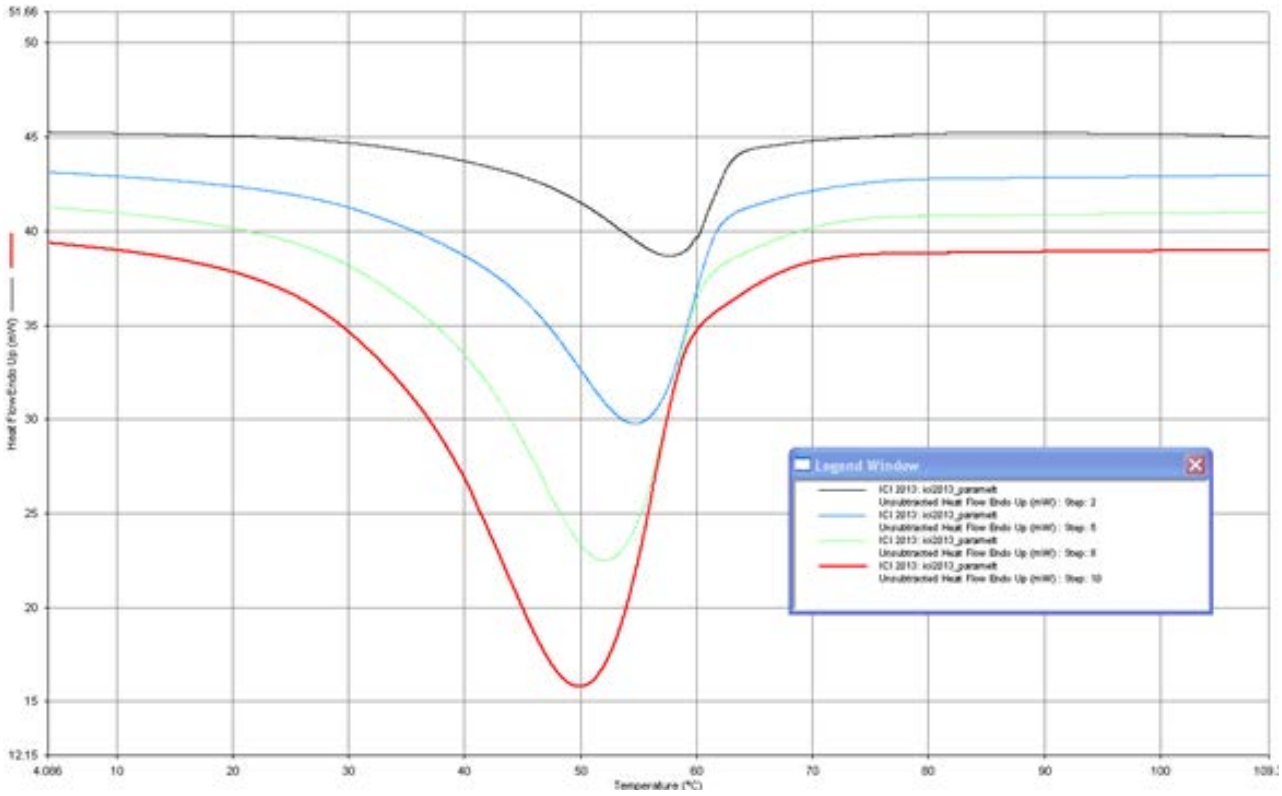

The DSC curves presented in Figure 5.6 for FastForm 20F shows evidence of at least two crystallization stages, possibly three. The shift in peak exotherm position is slightly less pronounced, and the position of the exotherm is, overall similar in temperature to that seen from Wax B despite its lower softening point. This also suggests that the early stages of crystallization found would have a lesser effect on the viscosity than with Wax B.

Figure 5.6. DSC traces from cooling of Wax C at different cooling rates.

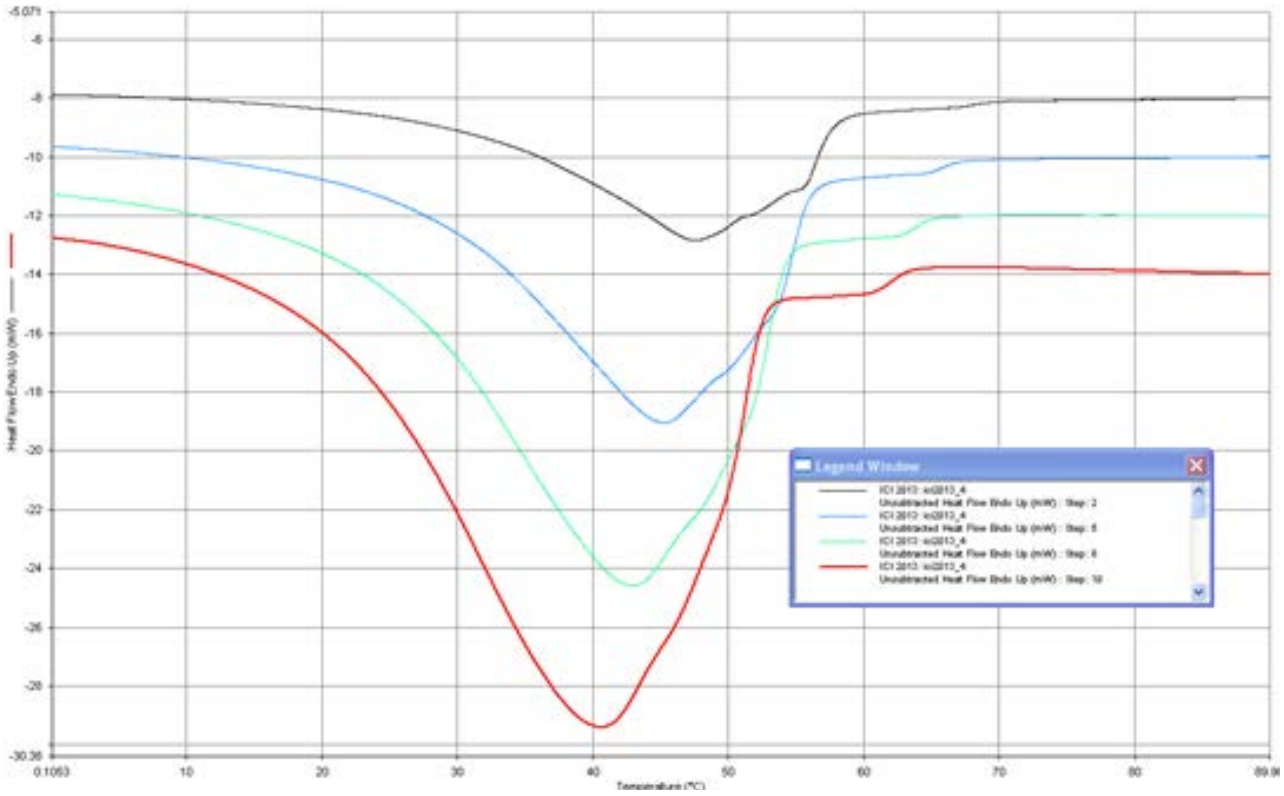

5.3 Results of DMA experiments.

Again considering Wax B, first, the DMA curve presented in Figure 5.7 shows that the wax undergoes little shrinkage from the softening point down to 50-55oC where the contraction begins in earnest.

Presented in Figure 5.8 are the overlaid displacement curves for Wax B and Wax C showing that the solid shrinkage of Wax C is slightly greater overall than the solid shrinkage of Wax B. The shrinkage starts earlier than the shrinkage for Wax B but they finish fairly closely together.

If we then add FastForm 20F to the plot, it can be seen that FastForm is remarkably similar to Wax B, despite the marked differences in the softening points of the wax. FastForm begins shrinkage a lot closer to the softening point.

Despite the major differences between the wax formulation (as determined by the pattern of the DSC curves), and their softening point differences, it would appear that the solid shrinkage of all three waxes are relatively similar.

Figure 5.7. Solid contraction of Wax B via DMA.

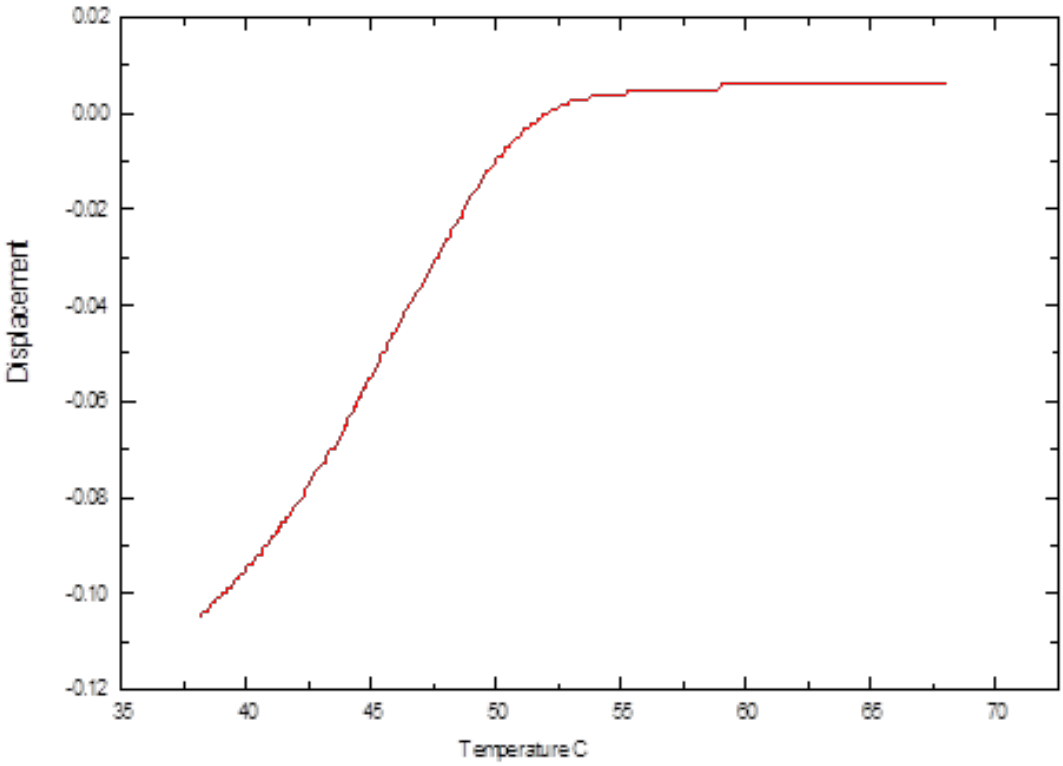

Figure 5.8. Overlaid DMA displacement curves for Wax B and Wax C.

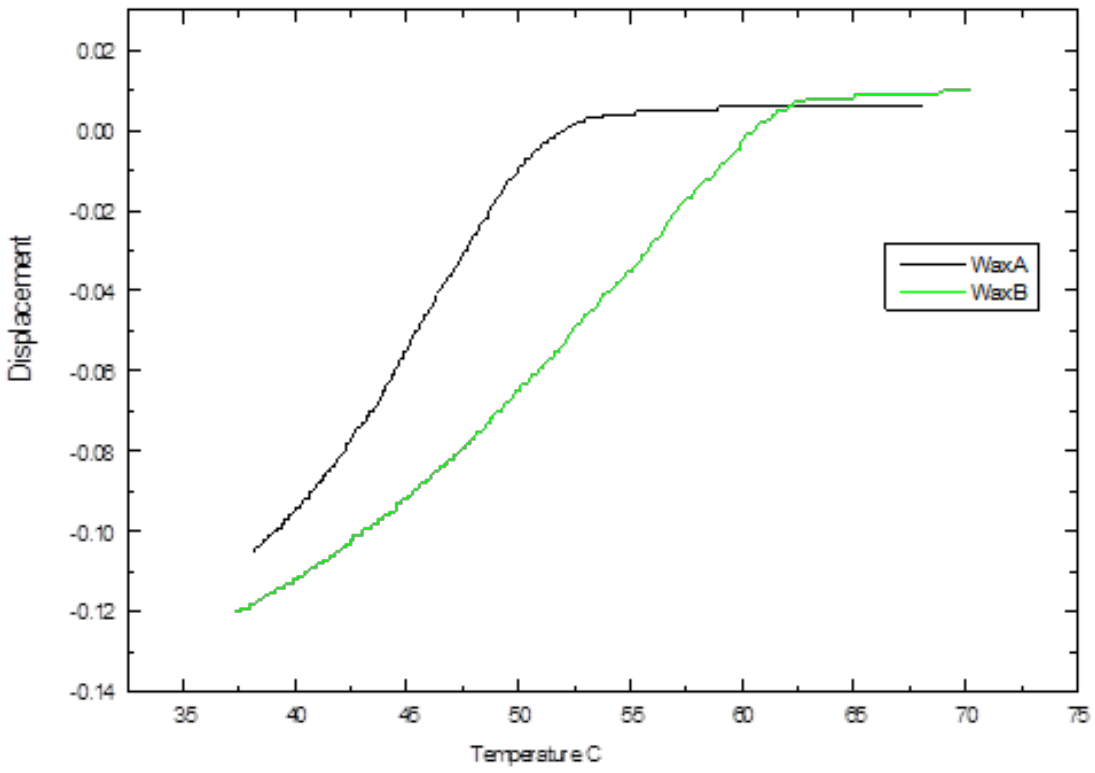

Figure 5.9. Overlaid DMA displacement curves for FastForm 20F, Wax B and C.

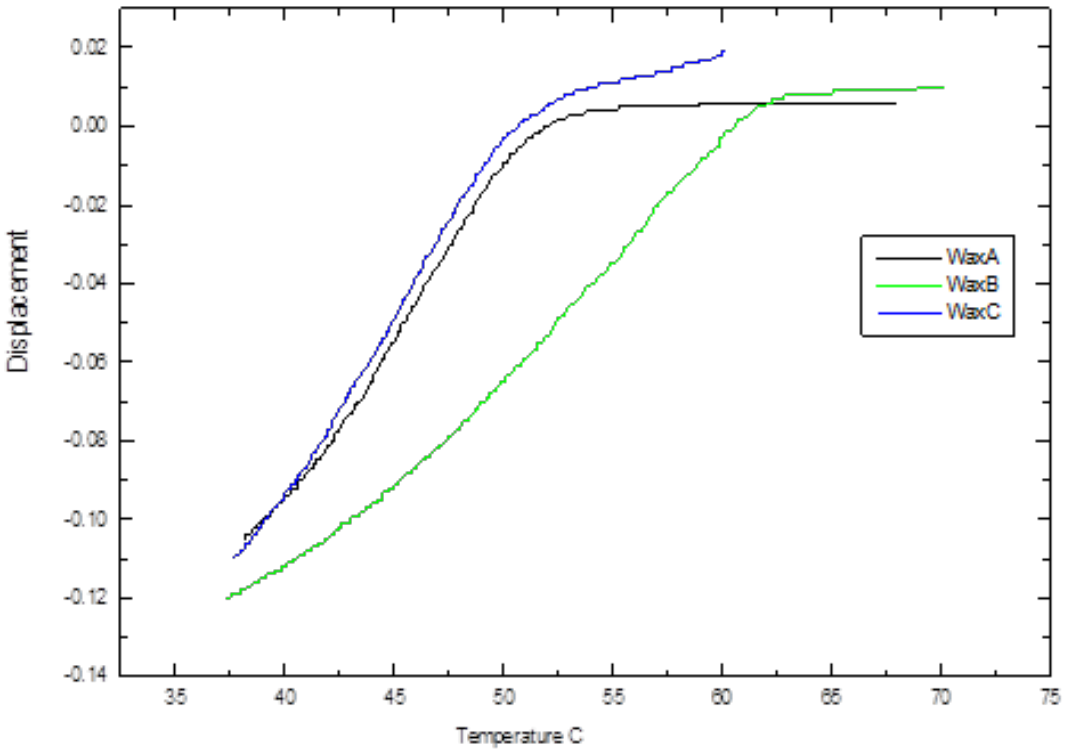

Despite the major differences between the wax formulation (as determined by the pattern of the DSC curves), and their softening point differences, it would appear that the solid shrinkage of all three waxes are relatively similar.

Control of the liquid (volumetric) shrinkage by adjustment of injection parameters could produce identical shrinkage for injected parts – provided the liquid properties of the wax are flexible enough!

At this point the evidence available suggests that the lower softening point and more flexible rheology characteristics of FastForm 20F ought to enable the development of injection parameters to match the overall shrinkage of either Wax B or Wax C.

But all these measurements presented in this section, while being subject to correlation with the real world, do not tell us anything about the finished wax part and how it will behave after it is removed from the tool. So the question must be asked, how similar are the properties of the finished, cooled, injected waxes?

5.4 Comparing Results of SCR, DSC, and DMA to Wax Injected Samples

The SCR, DSC and DMA studies carried out on the FastForm 20F along with Wax B and Wax C were conducted at the Remet UK laboratories support data obtained on viscosity measurements using industry standard measurement techniques and that observed shrinkage as function of dwell time.

Results of DOE experiments on injected wax samples can be summarized as follows:

1. Overall shrinkage of wax samples is very much dependent on wax injection temperature, as is well known.
2. Dwell time (length of time to inject tool plus hold time under injected pressure) does effect the overall shrinkage of wax samples.
3. Injection pressure and die temperature have very little effect on shrinkage.
4. Reduction in dwell time of nearly 40% was achieved with FastForm 20F to achieve the same minimum shrinkage as that of the 30% BPA filled Wax B.
5. FastForm and Wax C have nearly identical rate of viscosity increase (from minimum melt viscosity), both 63% higher than that of wax C.
6. FastForm has nearly 10 °C lower congealing point compared to Wax B (73 °C) and Wax C (74 °C).

So despite the major differences between the wax formulation (as determined by the pattern of the DSC curves) key properties, i.e. the congealing point, for a given shrinkage (or targeted dimension), there is a difference in the solid shrinkage of all three waxes tested.

While control of the wax injection temperature and dwell time are key to providing dimensionally accurate patterns, the lower congealing point of FastForm 20F and faster set up will permit faster throughput while meeting dimensional requirements of higher filled wax. This in turn may allow the production of shells with reduction in coating thickness while minimizing cracking.

6. Conclusion

The first thing to say is that the behaviour of FastForm is, overall, fairly different from the other two waxes. The solid shrinkage results from DMA show the same overall shrinkage as waxes containing substantially higher filler content which FastForm is designed to achieve.

This suggests that onset of crystallization plays a role in reducing the amount of volumetric change for a given proportion of liquid wax. This is despite the fact that some of the physical properties of the finished wax are close enough that transition, say, from Wax B to FastForm 20F might not cause issues with mechanical handling or wax tree resilience. Further work is underway on deflection and MOR testing to ensure that FastForm can meet the load and stability requirements during assembly and shell build of higher filled waxes.

The second major conclusion is that it would be very easy to mis-judge FastForm based on a limited or unoptimised trial. The rheology, DMA shrinkage and DSC results point to a wax that is not doing business as usual. This is especially true in the light of the traditional wax property measurements.

Accommodating these differences in production is going to take more than the typical put-the-wax-in-the-press-and-adjust-the settings approach. Suffice to say, the results of the DOE injection study suggest that a reduction in dwell time of up to 40% is possible with FastForm when patterns are injected at the lowest temperature feasible with while attaining complete fill and good surface finish.

The adoption of computer modelling systems in Europe to simulate wax injection, is an emerging tool to optimise the usage of existing waxes. It would be well worthwhile adopting a similar approach to get the best out of FastForm 20F.

In most industries, evolution is better accepted than revolution, mainly because it is less risky to adopt an evolutionary strategy and adapt the product to the process.
In this particular instance, adapting the process to the product might reap the best benefits.

7. Acknowledgements

The authors wish to acknowledge J. Siedlecki and N. Ossont for their technical assistance with conducting the wax injection experiments and obtaining material property data reported in this paper and to K. Zuis for technical discussions.

8. References

1. B. Phipps, “Digital Technology in the Wax Room”, Proceedings of the ICI 59th Annual Technical Conference & Expo, Nashville, TN, USA, October 8, 2012

2. H. Monks, Ph.d., “Flow and Deformation of Casting Waxes in the Solidification Region”, Proceedings of the ICI 8th World Conference on Investment Casting, London, UK, 28-30 June 1993.

3. G. Bradley, “Kinetics vs Thermodynamics: How Equilibrium States are Established in Investment Casting Waxes”, Proceedings of the ICI 59th Annual Technical Conference & Expo, Nashville, TN, USA, October 8, 2012.

[Blank Page]

Remet UK Ltd
44 Riverside II
Sir Thomas Longley Road
Rochester
Kent ME2 4DP

www.remetuk.com

Registered No. 478 0567 England